



UNIVERSITY
OF WOLLONGONG
AUSTRALIA

University of Wollongong
Research Online

Australian Institute for Innovative Materials - Papers

Australian Institute for Innovative Materials

2008

La and Nb codoped BiFeO₃ multiferroic thin films on LaNiO₃/Si and IrO₂/Si substrates

Zhenxiang Cheng

University of Wollongong, cheng@uow.edu.au

Xiaolin Wang

University of Wollongong, xiaolin@uow.edu.au

Hideo Kimura

National Institute for Materials Science, Japan

Kiyoshi Ozawa

National Institute for Materials Science, Japan, ozawa@uow.edu.au

S X. Dou

University of Wollongong, shi@uow.edu.au

Publication Details

Cheng, Z, Wang, X, Kimura, H, Ozawa, K & Dou, S (2008), La and Nb codoped BiFeO₃ multiferroic thin films on LaNiO₃/Si and IrO₂/Si substrates, *Applied Physics Letters*, 92(9), pp. 092902-1-092902-3.

Research Online is the open access institutional repository for the University of Wollongong. For further information contact the UOW Library:
research-pubs@uow.edu.au

La and Nb codoped BiFeO₃ multiferroic thin films on LaNiO₃/Si and IrO₂/Si substrates

Abstract

Nb and La codoped BiFeO₃ thin films were fabricated on oxide bottom electrodes, LaNiO₃/Si and IrO₂/Si, by pulsed laser deposition method. The doped BiFeO₃ thin film capacitor on LaNiO₃ showed a remnant polarization of more than 75 $\mu\text{C}/\text{cm}^2$ in a saturated hysteresis loop. The same La and Nb codoped BiFeO₃ thin film capacitors on IrO₂ showed a larger remnant polarization, while with a significant contribution from the leakage current. Furthermore, the doped BiFeO₃ capacitor on the LaNiO₃ bottom electrode showed worse fatigue resistance than the film on IrO₂. All the doped BiFeO₃ thin films showed weak ferromagnetism at room temperature.

Keywords

codoped, BiFeO₃, multiferroic, thin, films, LaNiO₃, IrO₂, substrates

Disciplines

Engineering | Physical Sciences and Mathematics

Publication Details

Cheng, Z, Wang, X, Kimura, H, Ozawa, K & Dou, S (2008), La and Nb codoped BiFeO₃ multiferroic thin films on LaNiO₃/Si and IrO₂/Si substrates, *Applied Physics Letters*, 92(9), pp. 092902-1-092902-3.

La and Nb codoped BiFeO₃ multiferroic thin films on LaNiO₃/Si and IrO₂/Si substrates

Z. X. Cheng,¹ X. L. Wang,^{1,a)} H. Kimura,² K. Ozawa,² and S. X. Dou¹

¹*Institute for Superconducting and Electronic Materials, University of Wollongong, New South Wales 2522, Australia*

²*National Institute for Material Science, 1-2-1 Sengen, Tsukuba, Ibaraki 305-0047, Japan*

(Received 16 January 2008; accepted 10 February 2008; published online 4 March 2008)

Nb and La codoped BiFeO₃ thin films were fabricated on oxide bottom electrodes, LaNiO₃/Si and IrO₂/Si, by pulsed laser deposition method. The doped BiFeO₃ thin film capacitor on LaNiO₃ showed a remnant polarization of more than 75 $\mu\text{C}/\text{cm}^2$ in a saturated hysteresis loop. The same La and Nb codoped BiFeO₃ thin film capacitors on IrO₂ showed a larger remnant polarization, while with a significant contribution from the leakage current. Furthermore, the doped BiFeO₃ capacitor on the LaNiO₃ bottom electrode showed worse fatigue resistance than the film on IrO₂. All the doped BiFeO₃ thin films showed weak ferromagnetism at room temperature. © 2008 American Institute of Physics. [DOI: 10.1063/1.2890068]

Multiferroic materials, displaying simultaneous magnetic and dipolar electrical orderings, have recently stimulated great scientific and technological interests. The coexistence of magnetic and electric subsystems endows materials with the “product” property, thus allowing an additional degree of freedom in the properties of actuators, sensors, and storage devices.^{1–7} However, the choice of single-phase materials that exhibit coexisting strong ferro/ferrimagnetism and ferroelectricity is limited.⁸ Among the rare single phase multiferroic materials, BiFeO₃, with a rhombohedrally distorted perovskite structure (space group *R3c*, $a=b=c=5.63$ Å, $\alpha=\beta=\gamma=59.4^\circ$), is the only known perovskite oxide that exhibits both antiferromagnetism (weak magnetism from canted spins or parasitic ferromagnetism like $\alpha\text{-Fe}_2\text{O}_3$) and ferroelectricity at room temperature (with Néel temperature $T_N \approx 643$ K and Curie temperature $T_C \approx 1103$ K).⁹ This material has recently attracted significant attention from the viewpoint of both fundamental research and the potential for practical applications involving mutual control of magnetization and polarization. Nevertheless, it has a serious electrical leakage problem, most likely as a result of sample defects, such as nonstoichiometry due to the volatility of bismuth during the fabrication of the thin film, oxygen vacancies, and variant valence states of the iron ions.¹⁰ Furthermore, the magnetic moment of the pure BiFeO₃ is very weak due to its antiferromagnetic nature. Great efforts have been focused on the improvement of both the ferroelectric and the magnetic properties.¹¹ Recently, the author reported that Nb and La codopings work effectively in reducing the electrical leakage of BiFeO₃ thin film on Pt/Ti/SiO₂/Si substrate, and a well-saturated electrical hysteresis loop with a sensing margin ($2P_r$) up to 160 $\mu\text{C}/\text{cm}^2$ was observed.¹² Furthermore, the magnetic moment of BiFeO₃ thin film is simultaneously improved by La doping. So the practical application of this codoped BiFeO₃ thin film as an element in various devices, especially for nonvolatile ferroelectric random access memory is very likely in the near future. Considering the wide range of applications and induced by the possible integration with other technology, for example, semiconductor

technology, various substrates and bottom electrodes are likely to be used for the deposition of the BiFeO₃ thin films. In this report, two oxide bottom electrodes were used for the deposition of La and Nb codoped BiFeO₃ thin films, and their ferroelectric and magnetic properties were studied.

The thin film samples in this work were deposited on two substrates, LaNiO₃/Si and IrO₂/Si, using a pulsed laser deposition system. Third harmonic generation of a Nd:yttrium aluminum garnet laser with a wavelength of 355 nm and a repetition rate of 10 Hz was used as the laser source. The targets, having compositions of Bi_{0.9}La_{0.1}Nb_{0.01}Fe_{0.99}O₃ (BLNF in short) with 5% excess bismuth, were synthesized by a standard solid-state reaction. The starting chemicals were Bi₂O₃, La₂O₃, Fe₃O₄, and Nb₂O₅ with purity of 99.9%, all supplied by Aldrich. The thin films were initially deposited on these substrates at 550 °C, then cooled down to room temperature following rapid thermal processing. During the deposition, the dynamic oxygen flow pressure was kept at 20 mTorr. The deposition conditions were kept the same for all the thin films on different substrates.

The phase and structure of the as-deposited films were determined by x-ray diffraction (XRD) using Cu $K\alpha$ radiation on a JEOL 3500 XRD machine. Pt upper electrodes with an area of 0.0314 mm² were deposited by magnetron sputtering through a metal shadow mask. The thicknesses of the films were measured by an optical reflection method with a Filmtek™ 4000 system from Scientific Computing International, USA. Results show that the two thin film samples studied in this report have a thickness of around 600 nm. The ferroelectric properties were measured at room temperature with an aixACCT EASY CHECK 300 ferroelectric tester. The dielectric properties of the thin films were measured using an HP4284 LCR meter. Magnetic properties of the thin film samples were investigated on a Quantum Design magnetic properties measurement system.

Figure 1 shows the x-ray diffraction pattern of the as-deposited thin films in comparison with that of the target bulk. All these thin films have the structure of single BiFeO₃ phase with space group *R3c*. Due to the differences in their structures, doped BiFeO₃ film on the two oxide substrates

^{a)}Electronic mail: xiaolin@uow.edu.au.

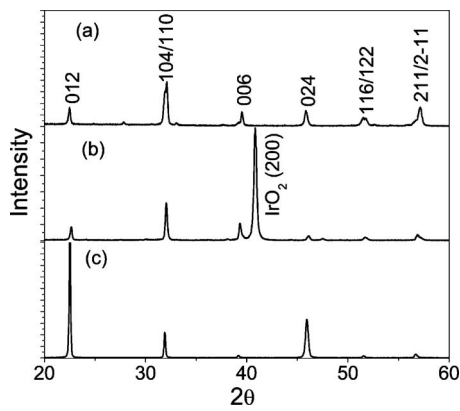


FIG. 1. Room temperature XRD patterns of the $\text{Bi}_{0.9}\text{La}_{0.1}\text{Nb}_{0.01}\text{Fe}_{0.99}\text{O}_3$ thin film deposited on oxide substrates in comparison with the target bulk: (a) target ceramics, (b) BLNF film on IrO_2/Si , and (c) BLNF film on LaNiO_3/Si .

shows different growth habits. The BLNF film on LaNiO_3/Si substrate shows strong (012) texture due to the lattice matching between BLNF (012) and LaNiO_3 (001). On IrO_2/Si substrate, no preferred growth habit was observed. The intensity ratio of the diffraction peaks is similar to that for the diffraction peaks of BiFeO_3 powder (PDF 74-2016) and the target bulk. It has been reported that, on $\text{Pt}/\text{Ti}/\text{SiO}_2/\text{Si}$ substrate, BLNF thin film shows a strong mixed (202) and (006) textures due to the lattice matching with Pt (111). Usually, the growth habits of the BLNF thin films depend not only on the substrates but also on the deposition conditions. With the same deposition conditions for these two thin film samples in this work, the growth habit only depends on the substrates. LaNiO_3 bottom electrode, having a perovskite structure, provides a better possibility for the epitaxial growth of the perovskite BiFeO_3 than the nonperovskite IrO_2 .

Figure 2 shows the ferroelectrical hysteresis loops of the BLNF thin film capacitors with a Pt top electrode and the two oxide bottom electrodes at room temperature. The BLNF thin film capacitor with LaNiO_3 as the bottom electrode shows well-saturated P - E loops, with a sensing margin of $2P_r = 150 \mu\text{C}/\text{cm}^2$ at the breakdown applied voltage. The ferroelectric performance of the BLNF film on IrO_2 substrate is somewhat different. No saturated P - E loop was obtained before the breakdown at high voltage. Although a very large sensing margin of $2P_r = 187 \mu\text{C}/\text{cm}^2$ was obtained below the breakdown voltage, a significant contribution from the leakage current was obvious, as evidenced by the round shape of the P - E loops, even at low voltage. This means that LaNiO_3 as the oxide electrode for BLNF thin film provides a better interface between the ferroelectric thin film and the electrode in terms of reducing leakage current. It should be noted that the P - E loops measured for the two samples all are apparently shifted toward positive field. Such a shift is often seen

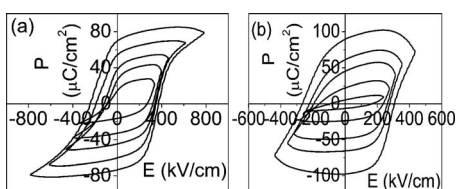


FIG. 2. Ferroelectric hysteresis loops of the $\text{Bi}_{0.9}\text{La}_{0.1}\text{Nb}_{0.01}\text{Fe}_{0.99}\text{O}_3$ thin film capacitors using Pt as the top electrode and different bottom electrodes: (a) LaNiO_3 and (b) IrO_2 measured at 100 Hz.

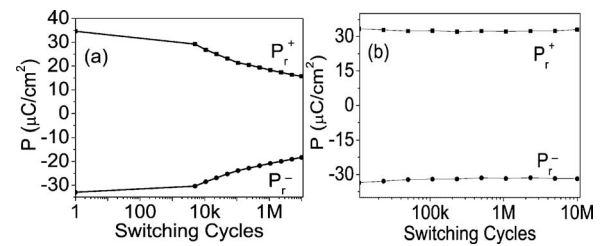


FIG. 3. Fatigue resistance measurement of the capacitors up to 10^7 switching cycles: (a) $\text{Pt}/\text{Bi}_{0.9}\text{La}_{0.1}\text{Nb}_{0.01}\text{Fe}_{0.99}\text{O}_3/\text{LaNiO}_3$ and (b) $\text{Pt}/\text{Bi}_{0.9}\text{La}_{0.1}\text{Nb}_{0.01}\text{Fe}_{0.99}\text{O}_3/\text{IrO}_2$. The measurement voltage was 25 V and switching voltage was 15 V with a frequency of 5 kHz.

in heteroepitaxial ferroelectric films and can be explained by the existence of an ultrathin interfacial layer, which results in an internal bias due to the accumulation of free charges at the interface between the ferroelectric and the nonswitching thin layer.¹³ Furthermore, the different bottom and top electrodes produce different interfacial layers close to the top and bottom electrodes, which causes the thin film capacitor to have an asymmetric structure and thus leads to asymmetric P - E loops. This shift was not observed for the BLNF thin film capacitor with Pt as both top and bottom electrodes.¹²

To further assess the ferroelectric performance of the BLNF thin films on oxide electrodes, fatigue resistance up to 10^7 switching cycles was measured at room temperature (shown in Fig. 3). The BLNF thin film capacitor using LaNiO_3 as the bottom electrode shows serious fatigue, with the remnant polarization dropping by up to 50% after 10^7 read and write cycles. However, for the BLNF thin film using IrO_2 as the bottom electrode, almost no fatigue was observed after 10^7 read and write cycles. The fatigue of the ferroelectric capacitors is related both to the ferroelectric thin film itself and to the electrode. There are several physical origins of the polarization fatigue effect, including domain wall pinning, formation of interfacial layers, and internal stress derived from 90° domains.¹⁴ As has been proved, BLNF thin film using Pt electrode shows a very strong fatigue resistance, which means that domain wall pinning is not significant inside the BLNF film.¹² It is likely that domain pinning caused by the movement and trapping of oxygen vacancies at the interfacial layer between the LaNiO_3 electrode and the BLNF film plays an important role in the weak fatigue resistance of BLNF film on LaNiO_3 electrode. The weak fatigue resistance strengthens the case for the existence of the interfacial layer that is evidenced by the shifting of the P - E loops in BLNF thin film on LaNiO_3 electrode. Although an interfacial layer probably exists between BLNF thin film and IrO_2 electrode and is suggested by the shifting of the P - E loops, this interfacial layer should have quite different physical properties, as evidenced by the larger current leakage in $\text{Pt}/\text{BLNF}/\text{IrO}_2$ capacitor than in $\text{Pt}/\text{BLNF}/\text{LaNiO}_3$ capacitor. In the $\text{Pt}/\text{BLNF}/\text{IrO}_2$ capacitor, the interfacial layer between BLNF film and IrO_2 electrode may provide a channel to conduct oxygen vacancies, hence preventing the large scale trapping of oxygen vacancies near the interfacial layer.

Figure 4 shows the magnetic properties of the BLNF thin films on the two different oxide bottom electrodes. The field cooled and zero-field cooled (FC-ZFC) magnetization processes revealed that all these thin films on different substrates had a weak magnetic moment with the transition tak-

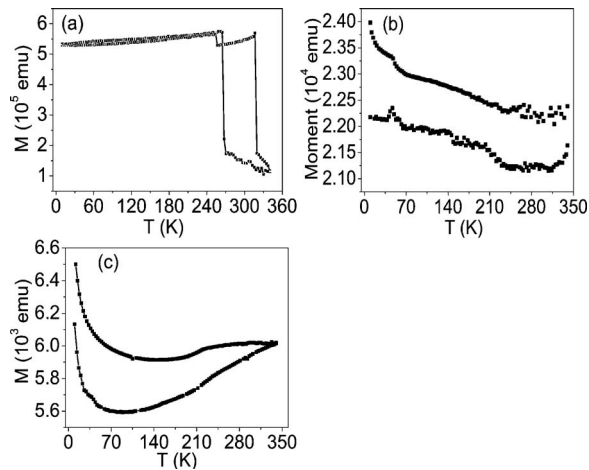


FIG. 4. Magnetization of the $\text{Bi}_{0.9}\text{La}_{0.1}\text{Nb}_{0.01}\text{Fe}_{0.99}\text{O}_3$ thin films on different electrodes: (a) LaNiO_3/Si , (b) IrO_2 , and (c) target bulk for comparison.

ing place above room temperature. This result is in accordance with the FC-ZFC magnetization measurements of the BLNF target bulk. For the BLNF thin film on LaNiO_3/Si substrate, an abrupt increase in the magnetic moment at around 270 K was observed. The origin of this abnormal feature needs further investigation. For the BLNF thin film on IrO_2 substrate, a sharp cusp was observed at around 50 K. Similarly, a weak cusp was also observed at a similar temperature in the FC-ZFC magnetization curve of the BLNF target bulk. This might be because a reorientation of the iron spin in the BLNF structure took place at low temperature. Alternatively, it might be due to domain wall pinning effects arising from local structure distortions.

In summary, La and Nb codoped BiFeO_3 thin films were fabricated on two oxide electrodes by the pulsed laser ablation method. The BLNF film using LaNiO_3 as the bottom electrode shows well-saturated P - E loops with large remnant polarization, but bad fatigue resistance. BLNF thin film using IrO_2 as the bottom electrode show worse P - E loops with serious current leakage, but better fatigue resistance. This

difference could be explained by the nature of the interfacial layer between the BLNF thin film and the bottom electrodes. However, in comparison to the BLNF thin film on Pt bottom electrode showing both good fatigue resistance and well-saturated P - E loops without obvious current leakage feature, the overall ferroelectric performance of the BLNF thin films on the two oxide bottom electrodes are not pleasant.¹² All of these thin film samples on oxide bottom electrodes are weakly ferromagnetic, with the transition occurring above room temperature.

The authors would like to thank the Australian Research Council (ARC) for support through Discovery projects (DP0558753 and DP0665873). We also thank Dr. Tania Silver for careful reading of this paper.

¹M. Fiebig, *J. Phys. D* **38**, R123 (2005).

²T. Goto, T. Kimura, G. Lawes, A. P. Ramirez, and Y. Tokura, *Phys. Rev. Lett.* **92**, 257201 (2004).

³T. Kimura, T. Goto, H. Shintani, K. Ishizaka, T. Arima, and Y. Tokura, *Nature (London)* **426**, 55 (2003).

⁴T. Lottermoser, T. Lonkai, U. Amann, D. Hohlwein, J. Ihringer, and M. Fiebig, *Nature (London)* **430**, 541 (2004).

⁵H. Ohno, D. Chiba, F. Matsukura, T. Omiya, E. Abe, T. Dietl, Y. Ohno, and K. Ohtani, *Nature (London)* **408**, 944 (2000).

⁶Z. X. Cheng and X. L. Wang, *Phys. Rev. B* **75**, 172406 (2007).

⁷N. Hur, S. Park, P. A. Sharma, J. S. Ahn, S. Guha, and S.-W. Cheong, *Nature (London)* **429**, 392 (2004).

⁸W. Prellier, M. P. Singh, and P. Murugavel, *J. Phys.: Condens. Matter* **17**, R803 (2005).

⁹J. Wang, J. B. Neaton, H. Zheng, V. Nagarajan, S. B. Ogale, B. Liu, D. Viehland, V. Vaithyanathan, D. G. Schlom, M. Wuttig, and R. Ramesh, *Science* **299**, 1719 (2003).

¹⁰Z. X. Cheng, X. L. Wang, S. X. Dou, H. Kimura, and K. Ozawa, *J. Appl. Phys.* (to be published).

¹¹Z. X. Cheng, X. L. Wang, C. V. Kannan, K. Ozawa, H. Kimura, and T. Nishida, *Appl. Phys. Lett.* **88**, 132909 (2006).

¹²Z. X. Cheng, X. L. Wang, H. Kimura, and K. Ozawa, *Phys. Rev. B* (to be published).

¹³J. Dho, X. Qi, H. Kim, J. L. MacManus-Driscoll, and M. G. Blamire, *Adv. Mater. (Weinheim, Ger.)* **18**, 1445 (2006).

¹⁴C. Verdier, F. D. Morrison, D. C. Lupascu, and J. F. Scott, *J. Appl. Phys.* **97**, 024107 (2005).